

# Criegee Intermediates React with Levoglucosan on Water

Shinichi Enami,\*,† Michael R. Hoffmann,† and A. J. Colussi

Supporting Information

ABSTRACT: Levoglucosan (Levo), a C<sub>6</sub>-anhydrosaccharide produced in the combustion of cellulosic materials, is the major component of aerosols produced from biomass burning over vast regions worldwide. Levo has long been considered chemically inert and thus has been used as a tracer of biomass burning sources. However, we now show that sugars including Levo, glucose, arabitol, and mannitol react rapidly with Criegee intermediates (CIs) generated during the ozonolysis of sesquiterpenes on the surface of water:acetonitrile microjets. Hydrophilic Levo reacts faster with CIs than with water or surface-active 1-octanol at air-aqueous interfaces. This

unexpected phenomenon is likely associated with the relatively low water density at air-aqueous interfaces coupled with a higher gas-phase acidity of the saccharide hydroxyl groups (i.e., -OH) versus n-alkanols. Results presented herein show that aerosol saccharides are in fact reactive toward CIs. Given the abundance of saccharides in the atmosphere, they may be important contributors to the growth and mass loading of secondary organic aerosols.

C accharides (sugars) are ubiquitous components of atmospheric particles generated from biomass burning. 1-8 Biomass is widely utilized as a domestic fuel worldwide such as in India, China, and various regions of Africa. The dense "brown aerosol" emitted from such sources absorbs and scatters sunlight, influencing climate $^{9-12}$  and affecting human health. 13,14 Field measurements of summertime aerosols over Mt. Tai, in the North China Plain, show that sugars are a dominant class of compounds throughout the campaign, with concentrations ranging from 49.8 to 2115 ng m<sup>-3</sup> (average 640 ng m $^{-3}$ ) in the daytime, and from 18.1 to 4348 ng m $^{-3}$  (799 ng m $^{-3}$ ) at night. Levoglucosan (Levo) $^{1,15}$  detected at 3432 ng m<sup>-3</sup> levels during the nighttime is the most abundant saccharide. Sugars are also present as water-soluble organic compounds in soils.4 From a chemical perspective, Levo and other sugars have been considered inert in the particle phase, except toward OH-radicals, 16-23 due to the absence of carbon carbon double bonds.

We recently found that Criegee intermediates (CIs, carbonyl oxide biradicals/zwitterions)<sup>24–27</sup> generated from the ozonolysis of sesquiterpenes ( $C_{15}H_{24}$ ,  $\beta$ -caryophyllene/ $\alpha$ -humulene) react with amphiphilic carboxylic acids rather than (H<sub>2</sub>O), in the outermost interfacial layers of water/acetonitrile mixtures. 28,29 This observation was ascribed to the low water concentrations prevalent in the outermost interfacial layers and the enrichment of the hydrophobic carboxylic acids therein. 28,29 We also reported that sesquiterpene CIs react with  $n \ge 4$ alcohols  $C_nH_{2n+1}OH$  to produce  $C_{15+n}$  ethers with yields that increase as a function of n.<sup>30</sup> The OH-group of 1-octanol proved to be  $\sim$ 25 times less reactive than the C(O)OH group of *n*-octanoic acid toward CIs at the air-liquid interface,

revealing that the reactivity of hydroxylic species therein depends both on their acidities and interfacial propensities.<sup>30</sup>

Here we demonstrate that sugars found in ambient aerosol and soils are very reactive with CIs at air-aqueous interfaces. We report the direct detection of initial products from reactions of Levo, glucose (Glu), arabitol (Ara), and mannitol (Man) with CIs generated on fresh surfaces of  $\beta$ -caryophyllene ( $\beta$ -C) and  $\alpha$ -humulene ( $\alpha$ -H) solutions in acetonitrile(AN):water(W) exposed to  $O_3(g)$  for ~10  $\mu$ s (Scheme 1).

Figure 1 shows negative ion electrospray mass spectrum of 1 mM  $\beta$ -C + 0.2 mM NaCl + 100 mM Levo in AN:W (4:1 = vol:vol) solution microjets in the absence and presence of  $O_3(g)$ . In the absence of  $O_3(g)$ , peaks appear at m/z 197;199 in the M/M+2 =  $3/1 = {}^{35}CI/{}^{37}CI$  ratio (Figure 1), that are assigned to chloride-Levo adducts  $(m/z \ 162 + 35/37 = 197/$ 199). The observation that neutral hydroxylic species form detectable chloride-adducts is in accordance with reports on the strong affinity of chloride for related species. 31-33 In the presence of  $O_3(g)$ , intense peaks appear at m/z 449;451 in addition to those at m/z 305;307 and 251. We confirmed that Levo is inert toward  $O_3(g)$  in the absence of  $\beta$ -C under the present condition (Figure S1), as expected from a structure lacking C=C double bonds. The m/z 449;451 corresponds to the products of Levo (MW = 162) addition to CIs: 449 (451) =204 + 48 + 162 + 35 (37) (Scheme 2).

The m/z 449;451 signals are assigned to the  $\alpha$ -alkoxyhydroperoxides (C<sub>21</sub> ethers) produced from the reaction of CIs

Received: June 29, 2017 Accepted: August 2, 2017 Published: August 2, 2017

<sup>&</sup>lt;sup>†</sup>National Institute for Environmental Studies, 16-2 Onogawa, Tsukuba, Ibaraki 305-8506, Japan

<sup>&</sup>lt;sup>‡</sup>Linde Center for Global Environmental Science, California Institute of Technology, Pasadena, California 91125, United States

Scheme 1. Structures of the Saccharides Used in the Present Study

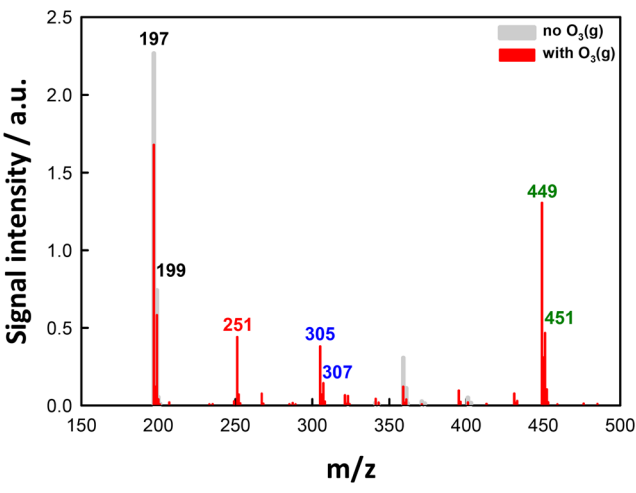
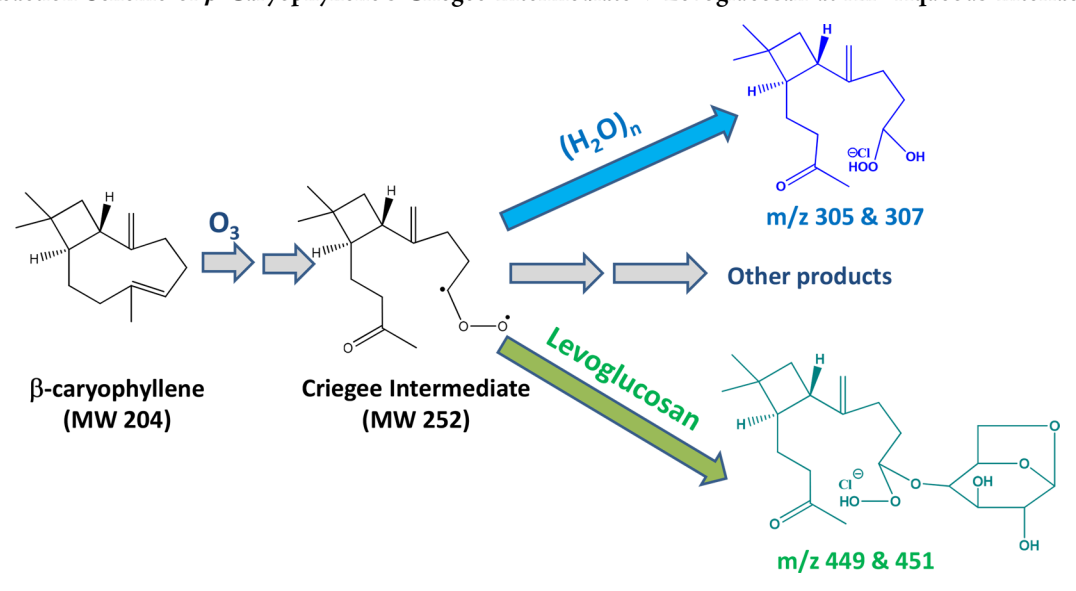


Figure 1. Negative ion electrospray mass spectra of 1 mM β-C + 0.2 mM NaCl + 100 mM levoglucosan in AN:W (4:1 = vol:vol) solution microjets (gray), or those exposed to  $O_3(g)$  (red,  $E=2.4\times10^{11}$  molecules cm<sup>-3</sup> s) at 1 atm and 298 K. The m/z 449;451 signals correspond to chloride-adducts of alkoxy-hydroperoxide products ( $C_{21}$  ether species) from the β-C's CIs + levoglucosan reaction. See the text for details.

with Levo. This result is surprising because CIs react faster with Levo than with interfacial  $(H_2O)_n$  at bulk molar ratios: [Levo]/ $[H_2O] = 100 \text{ mM}/23 \text{ M} \sim 4 \times 10^{-3} \text{ (molar fraction of } H_2O = 100 \text{ m}/23 \text{ m} \text{ m}/23 \text{ m}/23$ 

0.42 in 4:1::AN:W). Since surface-tension data suggests poly hydroxylic Levo is not surface-active, 34 this result implies that Levo has an exceptional intrinsic reactivity toward CIs at the air—water interface (see below). The m/z 305;307 and 251 corresponds to species resulting from the addition of  $O_3$  (+ 48) to a  $\beta$ -C (MW = 204) endo C=C bond, <sup>35,36</sup> followed by H<sub>2</sub>O addition (+18), which are detected as chloride-adducts (+35 or +37), i.e., 305(307) = 204 + 48 + 18 + 35(37), and functionalized-carboxylates, respectively (see our previous reports). 28-30 Clearly, Levo competes with interfacial water for CIs to generate a high mass product (MW 414, detected as m/z 449 and 451) versus the m/z = 305  $\alpha$ -hydroxyhydroperoxides from the reaction of CIs with (H<sub>2</sub>O)<sub>n</sub>. We previously found that the reactivities of CIs toward OH-species at the gas-liquid interface are positively correlated with their gas-phase acidities  $\Delta G_{
m acidity}$  (rather than with bond dissociation energies).30 This finding represents evidence of the participation of polar transition states involving zwitterionic rather than biradical CIs both in the gas-phase<sup>37</sup> and at air-aqueous interfaces.<sup>30</sup> Among the three –OH groups in Levo, the –OH groups at positions 1 and 3 (see Scheme 1) are significantly more acidic than that at position 2:  $\Delta G_{\text{acidity,#1}} = 1454$ ,  $\Delta G_{\text{acidity,#3}} = 1457 \text{ versus } \Delta G_{\text{acidity,#2}} = 1486 \text{ kJ mol}^{-1} \text{ (within 4 kJ mol}^{-1} \text{ accuracy),}^{38} \text{ and thus they will preferentially H-}$ transfer to the more negative terminal O atoms of CIs carbonyl oxides. On this basis, we tentatively propose the structure of the likely isomer shown for the m/z 449;451 product (Scheme 2).

Scheme 2. Reaction Scheme of  $\beta$ -Caryophyllene's Criegee Intermediate + Levoglucosan at Air-Aqueous Interfaces<sup>a</sup>



<sup>&</sup>lt;sup>a</sup>Here we show the most likely structures among possible isomers (see text).

Theoretical calculations might help pinpoint actual molecular structures, an issue that is beyond the scope of this paper.

Similar products at  $m/z = 204 + 48 + \text{MW}(\text{sugars}) + 35;37 = 467;469 (C_{21} \text{ ethers})$ , 439;441 (C<sub>20</sub> ethers), and 469;471 (C<sub>21</sub> ethers) are observed from the ozonolyses of  $\beta$ -C in the presence of Glu, Ara, and Man, respectively (Figures S2, S3, and S4). Interestingly, the signal intensities of ether products relative to that of the  $\alpha$ -hydroxy-hydroperoxide (m/z 305;307) are in the order: Ara > Levo ~ Man ~ Glu. This implies that that Ara is ~4 times more reactive than the other sugars on a molar basis (Figures S2, S3, and S4). The significantly higher reactivity of the C<sub>5</sub>- versus the C<sub>6</sub>-polyols toward CIs at the air—water interface suggests the operation of the subtle conformational effects predicted by recent calculations. <sup>39–42</sup>

Peaks at 449;451 appear both in the ozonolysis of  $\beta$ -C and  $\alpha$ -H in the presence of Levo (Figure S5). Also, peaks at 467;469, 439;441, and 469;471 are observed as major products from the ozonolyses of  $\alpha$ -H in the presence of Glu, Ara, and Man, respectively (Figures S6, S7, and S8). These results imply that sesquiterpene CIs will generally react with sugars at air—aqueous interfaces.

Additional evidence for the functionalities of the products was obtained in experiments involving isotopic labeling. Figure 2 and Figure S9 show negative ion electrospray mass spectra of

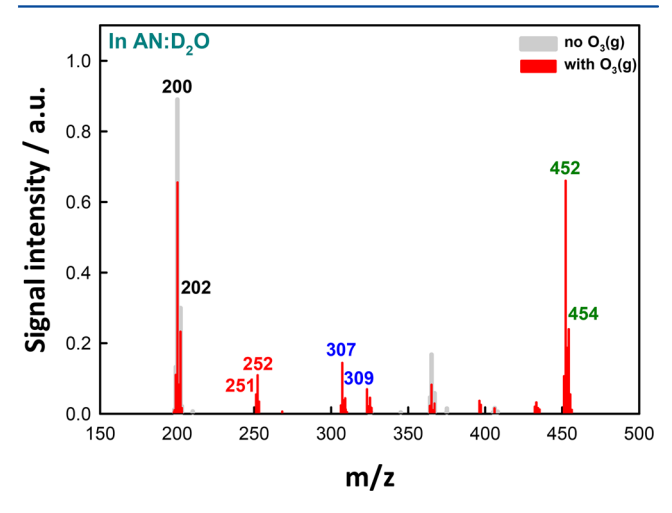


**Figure 2.** Negative ion electrospray mass spectra of 1 mM  $\beta$ -C + 0.5 mM NaCl + 100 mM levoglucosan in AN:D<sub>2</sub>O (4:1 = vol:vol) solution microjets (gray), or those exposed to O<sub>3</sub>(g) (red,  $E = 2.4 \times 10^{11}$  molecules cm<sup>-3</sup> s).

[ $\beta$ -C + NaCl + Levo] in AN:D<sub>2</sub>O and AN:H<sub>2</sub><sup>18</sup>O solution microjets in the absence and presence of O<sub>3</sub>(g). Chloride-Levo adducts (m/z 197;199) shifts to +3 mass units into 200;202 in AN:D<sub>2</sub>O (Figure 2), which is consistent with a structure having three exchangeable -O(H) groups. The fact that the m/z = 449;451 product signals do not shift in AN:H<sub>2</sub><sup>18</sup>O (Figure S9) is consistent with the formation of  $\alpha$ -alkoxy-hydroperoxides without the participation of water molecules (see Scheme 2). In contrast, the m/z 305;307 product signals shift by +2 mass units into 307;309 signals in both AN:D<sub>2</sub>O (Figure 2) and AN:H<sub>2</sub><sup>18</sup>O (Figure S9), in accordance with the formation of  $\alpha$ -hydroxy-hydroperoxides directly from the CIs + (H<sub>2</sub>O)<sub>n</sub> reaction (Scheme 2), as confirmed before. <sup>28–30</sup> The m/z 251 and 252 corresponds to keto- and aldehydic-carboxylates, respectively. <sup>28,35</sup> Note that since hydrophobic ether products (MW 414, detected as m/z 449;451 for Levo) still have one

(for  $\beta$ -C) and two (for  $\alpha$ -H) C=C double bond(s), their atmospheric processing would involve further ozonolysis into species possessing higher O/C ratios at the interface. More importantly, ethers containing labile hydroperoxide –OOH groups could trigger further oligomerizations.  $^{31,43-47}$  Such processes may underlie recent findings of extremely low-volatility organic compounds (ELVOCs) in a variety of field studies.  $^{48,49}$ 

Figure 3 shows electrospray mass spectral signals acquired from 1 mM  $\beta$ -C + 0.2 mM NaCl + 100 mM Levo in AN:W

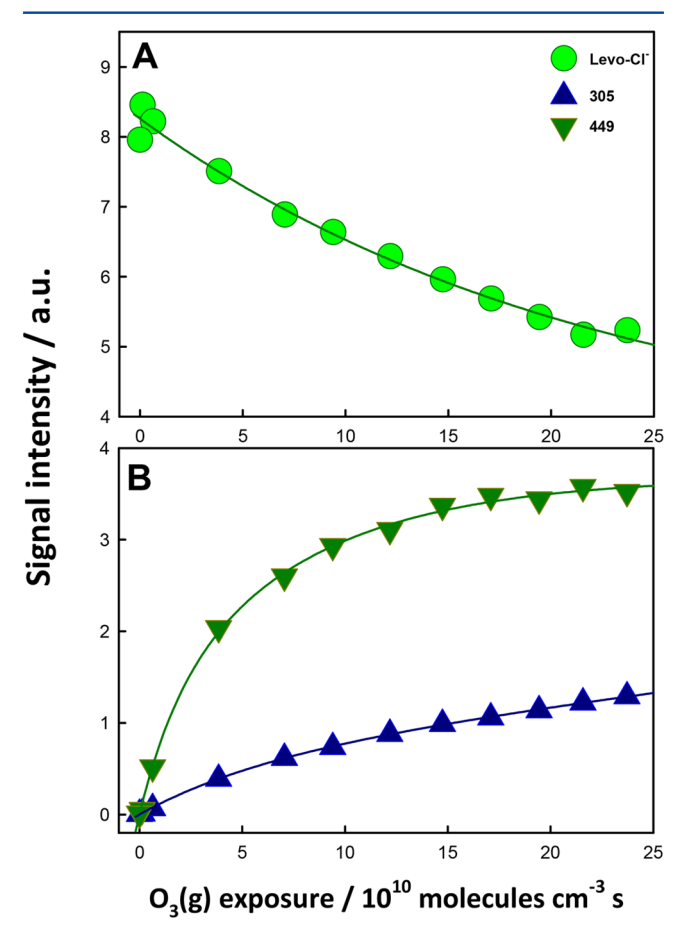


**Figure 3.** Reactant (A) and products (B) mass spectral signal intensities from 1 mM  $\beta\text{-C} + 0.2$  mM NaCl + 100 mM levoglucosan in AN:W (4:1 = vol:vol) solution microjets exposed to  $O_3(g)$  as functions of  $O_3(g)$  exposure (in  $10^{10}$  molecules cm $^{-3}$ s). The lines are regression curves fitted with double exponential decay or growth functions.

(4:1 = vol:vol) microjets exposed to gaseous  $O_3/O_2$  mixtures as functions of  $O_3(g)$  exposure. Product signals display nonzero initial slopes, suggesting that these are early major products generated in a few microseconds. Recent studies on AN:W binary mixtures revealed the microheterogeneity of their outermost interfacial layers, which are sparsely populated by disjoint water clusters in the molar fraction range relevant to our results.  $^{50,51}$ 

We quantified the competition between Levo and water at the gas—liquid interface by plotting the 449/305 signals ratio as a function of Levo concentration at constant  $O_3$  exposure (Figure 4). The linear rather than Langmuirian dependence on [Levo] observed in Figure 4 implies that the surface is never saturated with Levo under our experimental conditions. This is

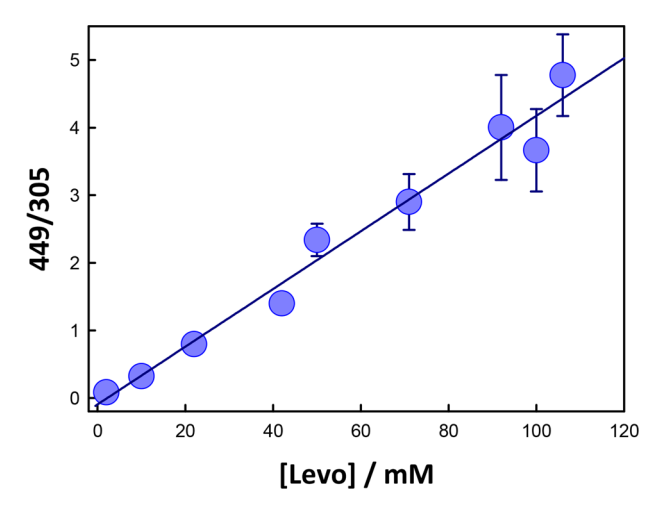


**Figure 4.** Ratio of 449/305 signal intensities as a function of concentration of levoglucosan in 1 mM β-caryophyllene + 0.2 mM NaCl in AN:H<sub>2</sub>O (4:1 = vol:vol) solution microjets exposed to O<sub>3</sub>(g),  $E = 2.4 \times 10^{11}$  molecules cm<sup>-3</sup> s. Error bars were derived from 2–5 independent experiments. The line is a linear-regression fitting.

consistent with reported surface-tension data on aqueous Levo solutions.<sup>34</sup> Notably, the slope in Figure 4 is larger than those from CIs + alkanoic acids/alkanols determined in our previous studies.<sup>28,30</sup>

The competition among hydrophilic Levo, interfacial water molecules and surface-active 1-octanol for CIs is shown in Figure 5. These experiments involve [1 mM  $\beta$ -C + 0.2 mM

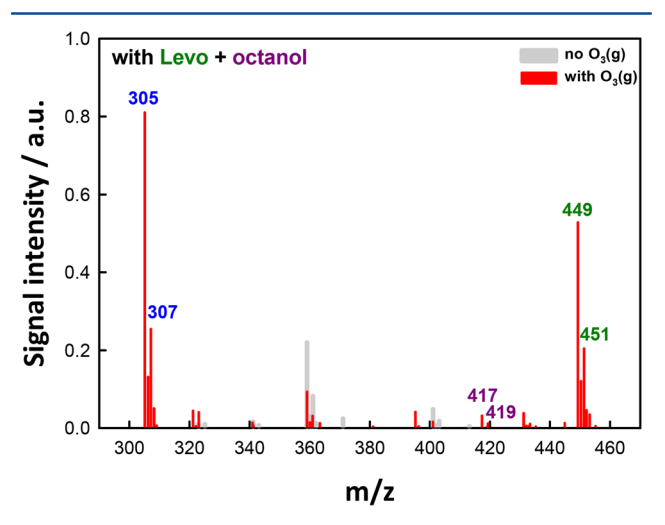


**Figure 5.** Negative ion electrospray mass spectra of [1 mM  $\beta$ -C + 0.2 mM NaCl + 100 mM Levo +100 mM 1-octanol] in AN:W (4:1 = vol:vol) solution microjets (gray), or those exposed to O<sub>3</sub>(g) (red,  $E=2.4\times10^{11}$  molecules cm<sup>-3</sup> s) at 1 atm and 298 K. The m/z 417;419 signals correspond to α-alkoxy-hydroperoxides from the CIs + 1-octanol reaction. See the text for details.

NaCl + 100 mM Levo + 100 mM 1-octanol (MW 130)] in AN:W (4:1 = vol:vol) solution microjets in the absence or presence of  $O_3(g)$ . The peaks at m/z 417;419 correspond to the products of 1-octanol addition to CIs: 417 (419) = 204 + 48 + 130 + 35 (37). Signal intensities at m/z 449;451 from CIs + Levo are ~20 times larger than those at m/z 417;419, implying that Levo is more reactive than 1-octanol toward CIs at the air—liquid interface. S2-56 We consider that the larger gasphase acidities of the multiple OH-groups of Levo and other

sugars, relative to linear monoalkanols underlie their exceptional reactivities toward CIs.  $^{38-41}$  Reported  $\Delta G_{\rm acidity}$  values for the different Levo –OH groups:  $\Delta G_{\rm acidity,\#1}=1454$ ,  $\Delta G_{\rm acidity,\#2}=1486$ ,  $\Delta G_{\rm acidity,\#3}=1457$  kJ mol $^{-1}$ , are significantly lower (i.e., –OH groups are more acidic) than those of n-alkanols  $C_nH_{2n+1}$ OH, which range from 1563 kJ mol $^{-1}$  (n=1) to 1525 kJ mol $^{-1}$  (n=8, 1-octanol), to but closer to those for n-alkanoic acids  $R_n$ -COOH: 1429 kJ mol $^{-1}$  (n=1) to 1418 kJ mol $^{-1}$  (n=6). As mentioned above, we recently reported that the reactivities of OH-species toward CIs are positively correlated with their gas-phase acidities  $\Delta G_{\rm acidity}$ . Mass spectra from the interfacial ozonolysis of [ $\beta$ -C + NaCl + Levo + octanoic acid (OA, MW 144)] also shows that signal intensities at m/z 449;451 from CIs + Levo are still  $\sim$ 2 times larger than the m/z 431;433 products from CIs + OA at [Levo] = [OA] = 100 mM (Figure S10). We infer that the multiple acidic -OH groups of Levo account for its enhanced reactivity towards CIs.

This study demonstrates that the ozonolysis of sesquiterpenes in the presence of atmospherically relevant sugars produce previously unreported large-mass α-alkoxy-hydroperoxides (C<sub>20</sub> or C<sub>21</sub> ether species) via "one-step" reactions on aqueous surfaces. Recent experimental studies have shown that Levo can also react with OH-radicals during the aging process, thereby casting doubts about its role as a biomass burning tracer. 16-23 Importantly, in contrast with OH-radical oxidations, C=C + O<sub>3</sub> + sugars reactions in/on aqueous organic aerosol occur during day- and night-time. We point out that unsaturated organic species, which are reactively uptaken via protonation on acidic pH < 4 aqueous surfaces,  $^{59-64}$  will be present as such on the very acidic atmospheric particles collected in recent field measurements. 65-70 Under such conditions, the CIs produced via interfacial ozonolysis (O<sub>3</sub> is rather insoluble in water, Henry's law constant H = 0.01 M atm<sup>-1</sup>) are expected to react with ubiquitous sugars or surfaceactive cis-pinonic acid, 29 rather than water and hydrophilic acids.

In summary, our experiments show that CIs produced by ozonolysis of sesquiterpenes react with atmospherically relevant saccharides in the interfacial layers of model aqueous organic aerosols. We provide mass-specific identification of the products generated in a very short (<10  $\mu$ s) reaction time-frames on fresh aqueous organic surfaces. Present results suggest that CIs will largely react with sugars rather than water molecules at air—aqueous interfaces. Therein, Levo is ~20 times more reactive than 1-octanol, and ~2 times more reactive than n-octanoic acid toward CIs. Our results reveal that sugars could be important, hitherto unrecognized, contributors to the growth/augmentation of atmospheric particles and play substantial roles in the troposphere.

# **EXPERIMENTAL SECTION**

We utilize sesquiterpene ( $\beta$ -C or  $\alpha$ -H) + saccharide (levoglucosan, glucose, arabitol or mannitol) in acetonitrile:water (AN:W = 4:1 = vol:vol) microjets into the spraying chamber of an electrospray mass spectrometer (ES-MS, Agilent 6130 Quadrupole LC/MS Electrospray System at NIES, Japan) flushed with N<sub>2</sub>(g) at 1 atm, 298 K. The experimental setup is essentially the same as those we reported elsewhere. We use sesquiterpenes as in situ sources of CIs due to their extreme reactivities toward O<sub>3</sub>(g), which makes them compatible with the short  $\tau_R \sim 10~\mu s$  contact times of our experiments. An AN:W mixture solvent is used as a suitable surrogate of atmospheric aqueous organic media because the composition of

its interfacial layers is well characterized both by theory and experiments. 50,51 Microjets are exposed to orthogonal gas-phase O<sub>3</sub>/O<sub>2</sub> beams. AN:W solutions containing reactants are pumped (100  $\mu$ L min<sup>-1</sup>) into the spraying chamber through a grounded stainless steel needle (100  $\mu$ m bore) coaxial with a sheath issuing nebulizer  $N_2(g)$  at a high gas velocity  $\nu_{\sigma}$  (~160 m sec<sup>-1</sup>).<sup>74</sup> The species detected by ES mass spectrometry are produced in collisions of gaseous O3 with the surface of the intact aqueous microjets just after they emerge from the nozzle.<sup>72</sup> The modest polarizations of the initial microjets do not affect the observed phenomena. These mass spectra correspond to species generated by heterogeneous processes in the outermost interfacial layers of initial microjets as shown in our previous studies.  $^{54,71,72}$  Present small ozone exposures: E = $[O_3(g)] \times \tau_R \le 2.4 \times 10^{11}$  molecules cm<sup>-3</sup> s enables us to monitor very early stages of CIs reactions on the liquid surface. In the presence of chloride anion, most of the negatively charged species we detect in our experiments correspond to chloride-adducts of neutrals, which are unambiguously identified by their characteristic M/M+2 = 3/1 ratio arising from the  ${}^{35}Cl/{}^{37}Cl$  ratio. Chloride is inert toward  $O_3(g)$  under present conditions as shown before. 28,77 Further experimental details could be found in previous publications.<sup>28,71,73</sup>

Ozone was generated by flowing ultrapure O2(g) (>99.999%) through a silent discharge ozonizer (KSQ-050, Kotohira, Japan) and quantified via online UV-vis absorption spectrophotometry (Agilent 8453) prior to entering the reaction chamber. The reported [O<sub>3</sub>(g)] values correspond to the concentrations actually sensed by the microjets in the reaction chamber that are estimated to be ~12 times smaller than the values determined from UV absorbance due to dilution by the drying nitrogen gas. Conditions in the present experiments were as follows: drying nitrogen gas flow rate: 12 L min<sup>-1</sup>; drying nitrogen gas temperature: 340 °C; inlet voltage: + 3.5 kV relative to ground; fragmentor voltage value: 60 V. All solutions were prepared in purified water (resistivity  $\geq 18.2 \text{ M}\Omega$ cm at 298 K) from a Millipore Milli-Q water purification system and used within a couple of days. Chemicals:  $\beta$ caryophyllene ( $\geq$ 98.5%, Sigma-Aldrich),  $\alpha$ -humulene ( $\geq$ 96.0%, Sigma-Aldrich), levoglucosan (≥99%, Sigma-Aldrich), D-(+)-glucose (ACS reagent, Sigma-Aldrich), D-(+)-arabitol (≥99.0%, Wako), D-mannitol (≥98%, Sigma-Aldrich), acetonitrile (≥99.8%, Wako), D<sub>2</sub>O (99.9 atom % D, Sigma-Aldrich),  $H_2^{18}O$  (97%, Santa Cruz Isotope), and NaCl ( $\geq$ 99.999%, Sigma-Aldrich) were used as received.

#### ASSOCIATED CONTENT

# S Supporting Information

The Supporting Information is available free of charge on the ACS Publications website at DOI: 10.1021/acs.jpclett.7b01665.

Additional experimental data (PDF)

## AUTHOR INFORMATION

## **Corresponding Author**

\*E-mail: enami.shinichi@nies.go.jp; phone: +81-29-850-2770.

ORCID

Shinichi Enami: 0000-0002-2790-7361 A. J. Colussi: 0000-0002-3400-4101

# **Author Contributions**

S.E. designed and performed research; S.E. and A.J.C. analyzed data; S.E., M.R.H., and A.J.C. wrote the paper.

#### **Notes**

The authors declare no competing financial interest.

## ACKNOWLEDGMENTS

We are grateful to Prof. Yosuke Sakamoto of Kyoto University, and Drs. Satoshi Inomata, Akihiro Fushimi, and Kei Sato of NIES for valuable discussions. This work is partly supported by the research foundation for opto-science and technology, JSPS KAKENHI Grant Numbers 15H05328 and 15K12188.

### REFERENCES

- (1) Fu, P. Q.; Kawamura, K.; Okuzawa, K.; Aggarwal, S. G.; Wang, G. H.; Kanaya, Y.; Wang, Z. F. Organic Molecular Compositions and Temporal Variations of Summertime Mountain Aerosols over Mt. Tai, North China Plain. *J. Geophys. Res.* **2008**, *113*, D19107.
- (2) Cheng, Y.; Brook, J. R.; Li, S. M.; Leithead, A. Seasonal Variation in the Biogenic Secondary Organic Aerosol Tracer Cis-Pinonic Acid: Enhancement Due to Emissions from Regional and Local Biomass Burning. *Atmos. Environ.* **2011**, *45*, 7105–7112.
- (3) Agarwal, S.; Aggarwal, S. G.; Okuzawa, K.; Kawamura, K. Size Distributions of Dicarboxylic Acids, Ketoacids, Alpha-Dicarbonyls, Sugars, WSOC, OC, EC and Inorganic Ions in Atmospheric Particles over Northern Japan: Implication for Long-Range Transport of Siberian Biomass Burning and East Asian Polluted Aerosols. *Atmos. Chem. Phys.* **2010**, *10*, 5839–5858.
- (4) Simoneit, B. R. T.; Elias, V. O.; Kobayashi, M.; Kawamura, K.; Rushdi, A. I.; Medeiros, P. M.; Rogge, W. F.; Didyk, B. M. Sugars: Dominant Water-Soluble Organic Compounds in Soils and Characterization as Tracers in Atmospheric Particulate Matter. *Environ. Sci. Technol.* **2004**, *38*, 5939–5949.
- (5) Kumar, S.; Aggarwal, S. G.; Fu, P. Q.; Kang, M.; Sarangi, B.; Sinha, D.; Kotnala, R. K. Size-Segregated Sugar Composition of Transported Dust Aerosols from Middle-East over Delhi During March 2012. *Atmos. Res.* **2017**, *189*, 24–32.
- (6) Liang, L. L.; Engling, G.; Du, Z. Y.; Cheng, Y.; Duan, F. K.; Liu, X. Y.; He, K. B. Seasonal Variations and Source Estimation of Saccharides in Atmospheric Particulate Matter in Beijing, China. *Chemosphere* **2016**, *150*, 365–377.
- (7) Li, X.; Jiang, L.; Hoa, L. P.; Lyu, Y.; Xu, T. T.; Yang, X.; Iinuma, Y.; Chen, J. M.; Herrmann, H. Size Distribution of Particle-Phase Sugar and Nitrophenol Tracers During Severe Urban Haze Episodes in Shanghai. *Atmos. Environ.* **2016**, *145*, 115–127.
- (8) Li, X.; Chen, M. X.; Le, H. P.; Wang, F. W.; Guo, Z. G.; Iinuma, Y.; Chen, J. M.; Herrmann, H. Atmospheric Outflow of PM2.5 Saccharides from Megacity Shanghai to East China Sea: Impact of Biological and Biomass Burning Sources. *Atmos. Environ.* **2016**, 143, 1–14.
- (9) Laskin, A.; Laskin, J.; Nizkorodov, S. A. Chemistry of Atmospheric Brown Carbon. *Chem. Rev.* **2015**, *115*, 4335–4382.
- (10) Lack, D. A.; Langridge, J. M.; Bahreini, R.; Cappa, C. D.; Middlebrook, A. M.; Schwarz, J. P. Brown Carbon and Internal Mixing in Biomass Burning Particles. *Proc. Natl. Acad. Sci. U. S. A.* **2012**, *109*, 14802—14807
- (11) Li, W. J.; Shao, L. Y.; Buseck, P. R. Haze Types in Beijing and the Influence of Agricultural Biomass Burning. *Atmos. Chem. Phys.* **2010**, *10*, 8119–8130.
- (12) Budisulistiorini, S. H.; Riva, M.; Williams, M.; Chen, J.; Itoh, M.; Surratt, J. D.; Kuwata, M. Light-Absorbing Brown Carbon Aerosol Constituents from Combustion of Indonesian Peat and Biomass. *Environ. Sci. Technol.* **2017**, *51*, 4415–4423.
- (13) Huang, R. J.; et al. High Secondary Aerosol Contribution to Particulate Pollution During Haze Events in China. *Nature* **2014**, *514*, 218–222.
- (14) Adler, G.; Flores, J. M.; Riziq, A. A.; Borrmann, S.; Rudich, Y. Chemical, Physical, and Optical Evolution of Biomass Burning Aerosols: A Case Study. *Atmos. Chem. Phys.* **2011**, *11*, 1491–1503.
- (15) Fu, P. Q.; Kawamura, K.; Kanaya, Y.; Wang, Z. F. Contributions of Biogenic Volatile Organic Compounds to the Formation of

- Secondary Organic Aerosols over Mt Tai, Central East China. Atmos. Environ. 2010, 44, 4817–4826.
- (16) Hennigan, C. J.; et al. Chemical and Physical Transformations of Organic Aerosol from the Photo-Oxidation of Open Biomass Burning Emissions in an Environmental Chamber. *Atmos. Chem. Phys.* **2011**, 11, 7669–7686.
- (17) Kessler, S. H.; Smith, J. D.; Che, D. L.; Worsnop, D. R.; Wilson, K. R.; Kroll, J. H. Chemical Sinks of Organic Aerosol: Kinetics and Products of the Heterogeneous Oxidation of Erythritol and Levoglucosan. *Environ. Sci. Technol.* **2010**, *44*, 7005–7010.
- (18) Hoffmann, D.; Tilgner, A.; Iinuma, Y.; Herrmann, H. Atmospheric Stability of Levoglucosan: A Detailed Laboratory and Modeling Study. *Environ. Sci. Technol.* **2010**, *44*, 694–699.
- (19) Hennigan, C. J.; Sullivan, A. P.; Collett, J. L.; Robinson, A. L. Levoglucosan Stability in Biomass Burning Particles Exposed to Hydroxyl Radicals. *Geophys. Res. Lett.* **2010**, *37*, L09806.
- (20) Zhao, R.; Mungall, E. L.; Lee, A. K. Y.; Aljawhary, D.; Abbatt, J. P. D. Aqueous-Phase Photooxidation of Levoglucosan A Mechanistic Study Using Aerosol Time-of-Flight Chemical Ionization Mass Spectrometry (Aerosol TOF-CIMS). *Atmos. Chem. Phys.* **2014**, *14*, 9695–9706.
- (21) Lai, C.; Liu, Y.; Ma, J.; Ma, Q.; He, H. Degradation Kinetics of Levoglucosan Initiated by Hydroxyl Radical under Different Environmental Conditions. *Atmos. Environ.* **2014**, *91*, 32–39.
- (22) Slade, J. H.; Knopf, D. A. Heterogeneous OH Oxidation of Biomass Burning Organic Aerosol Surrogate Compounds: Assessment of Volatilisation Products and the Role of OH Concentration on the Reactive Uptake Kinetics. *Phys. Chem. Chem. Phys.* **2013**, *15*, 5898–5915.
- (23) Holmes, B. J.; Petrucci, G. A. Oligomerization of Levoglucosan by Fenton Chemistry in Proxies of Biomass Burning Aerosols. *J. Atmos. Chem.* **2007**, *58*, 151–166.
- (24) Miliordos, E.; Xantheas, S. S. The Origin of the Reactivity of the Criegee Intermediate: Implications for Atmospheric Particle Growth. *Angew. Chem., Int. Ed.* **2016**, *55*, 1015–1019.
- (25) Osborn, D. L.; Taatjes, C. A. The Physical Chemistry of Criegee Intermediates in the Gas Phase. *Int. Rev. Phys. Chem.* **2015**, *34*, 309–360.
- (26) Lee, Y. P. Perspective: Spectroscopy and Kinetics of Small Gaseous Criegee Intermediates. J. Chem. Phys. 2015, 143, 020901.
- (27) Nakajima, M.; Endo, Y. Communication: Determination of the Molecular Structure of the Simplest Criegee Intermediate CH<sub>2</sub>OO. *J. Chem. Phys.* **2013**, 139, 101103.
- (28) Enami, S.; Colussi, A. J. Criegee Chemistry on Aqueous Organic Surfaces. J. Phys. Chem. Lett. 2017, 8, 1615–1623.
- (29) Enami, S.; Colussi, A. J. Efficient Scavenging of Criegee Intermediates on Water by Surface-Active Cis-Pinonic Acid. *Phys. Chem. Chem. Phys.* **2017**, *19*, 17044–17051.
- (30) Enami, S.; Colussi, A. J. Reactions of Criegee Intermediates with Alcohols at Air-Aqueous Interfaces. *J. Phys. Chem. A* **2017**, *121*, 5175–5182.
- (31) Sakamoto, Y.; Inomata, S.; Hirokawa, J. Oligomerization Reaction of the Criegee Intermediate Leads to Secondary Organic Aerosol Formation in Ethylene Ozonolysis. *J. Phys. Chem. A* **2013**, *117*, 12912—12921.
- (32) Larson, J. W.; McMahon, T. B. Fluoride and Chloride Affinities of Main Group Oxides, Fluorides, Oxofluorides, and Alkyls. Quantitative Scales of Lewis Acidities from Ion Cyclotron Resonance Halide-Exchange Equilibria. *I. Am. Chem. Soc.* **1985**, *107*, 766–773.
- (33) Bohringer, H.; Fahey, D. W.; Fehsenfeld, F. C.; Ferguson, E. E. Bond-Energies of the Molecules H<sub>2</sub>O, SO<sub>2</sub>, H<sub>2</sub>O<sub>2</sub>, and HCl to Various Atmospheric Negative-Ions. *J. Chem. Phys.* **1984**, *81*, 2805–2810.
- (34) Tuckermann, R.; Cammenga, H. K. The Surface Tension of Aqueous Solutions of Some Atmospheric Water-Soluble Organic Compounds. *Atmos. Environ.* **2004**, *38*, 6135–6138.
- (35) Enami, S.; Hoffmann, M. R.; Colussi, A. J. Prompt Formation of Organic Acids in Pulse Ozonation of Terpenes on Aqueous Surfaces. *J. Phys. Chem. Lett.* **2010**, *1*, 2374–2379.

- (36) Winterhalter, R.; Herrmann, F.; Kanawati, B.; Nguyen, T. L.; Peeters, J.; Vereecken, L.; Moortgat, G. K. The Gas-Phase Ozonolysis of Beta-Caryophyllene ( $C_{15}H_{24}$ ). Part I: An Experimental Study. *Phys. Chem. Chem. Phys.* **2009**, *11*, 4152–4172.
- (37) Tobias, H. J.; Ziemann, P. J. Kinetics of the Gas-Phase Reactions of Alcohols, Aldehydes, Carboxylic Acids, and Water with the C13 Stabilized Criegee Intermediate Formed from Ozonolysis of 1-Tetradecene. *J. Phys. Chem. A* **2001**, *105*, 6129–6135.
- (38) Rocha, I. M.; Galvão, T. L. P.; Sapei, E.; Ribeiro da Silva, M. D. M. C.; Ribeiro da Silva, M. A. V. Levoglucosan: A Calorimetric, Thermodynamic, Spectroscopic, and Computational Investigation. *J. Chem. Eng. Data* **2013**, *58*, 1813–1821.
- (39) Salpin, J. Y.; Tortajada, J. Gas-Phase Acidity of D-Glucose. A Density Functional Theory Study. *J. Mass Spectrom.* **2004**, 39, 930–941
- (40) Yang, G.; Zhu, C.; Zhou, L. J. Deprotonation and Acidity Characterization of Biomass Sugars: A First-Principles Study. *J. Mol. Model.* **2016**, 22, 10.
- (41) Feng, S. T.; Bagia, C.; Mpourmpakis, G. Determination of Proton Affinities and Acidity Constants of Sugars. *J. Phys. Chem. A* **2013**, 117, 5211–5219.
- (42) Vereecken, L.; Harder, H.; Novelli, A. The Reactions of Criegee Intermediates with Alkenes, Ozone, and Carbonyl Oxides. *Phys. Chem. Chem. Phys.* **2014**, *16*, 4039–4049.
- (43) Sakamoto, Y.; Yajima, R.; Inomata, S.; Hirokawa, J. Water Vapour Effects on Secondary Organic Aerosol Formation in Isoprene Ozonolysis. *Phys. Chem. Chem. Phys.* **2017**, *19*, 3165–3175.
- (44) Riva, M.; Budisulistiorini, S. H.; Zhang, Z.; Gold, A.; Thornton, J. A.; Turpin, B. J.; Surratt, J. D. Multiphase Reactivity of Gaseous Hydroperoxide Oligomers Produced from Isoprene Ozonolysis in the Presence of Acidified Aerosols. *Atmos. Environ.* **2017**, *152*, 314–322.
- (45) Wang, M. Y.; Yao, L.; Zheng, J.; Wang, X. K.; Chen, J. M.; Yang, X.; Worsnop, D. R.; Donahue, N. M.; Wang, L. Reactions of Atmospheric Particulate Stabilized Criegee Intermediates Lead to High-Molecular-Weight Aerosol Components. *Environ. Sci. Technol.* **2016**, *50*, 5702–5710.
- (46) Tong, H.; Arangio, A. M.; Lakey, P. S. J.; Berkemeier, T.; Liu, F.; Kampf, C. J.; Brune, W. H.; Pöschl, U.; Shiraiwa, M. Hydroxyl Radicals from Secondary Organic Aerosol Decomposition in Water. *Atmos. Chem. Phys.* **2016**, *16*, 1761–1771.
- (47) Vidrio, E.; Phuah, C. H.; Dillner, A. M.; Anastasio, C. Generation of Hydroxyl Radicals from Ambient Fine Particles in a Surrogate Lung Fluid Solution. *Environ. Sci. Technol.* **2009**, 43, 922–927
- (48) Barsanti, K. C.; Kroll, J. H.; Thornton, J. A. Formation of Low-Volatility Organic Compounds in the Atmosphere: Recent Advancements and Insights. *J. Phys. Chem. Lett.* **2017**, *8*, 1503–1511.
- (49) Kristensen, K.; Watne, Å. K.; Hammes, J.; Lutz, A.; Petäjä, T.; Hallquist, M.; Bilde, M.; Glasius, M. High-Molecular Weight Dimer Esters Are Major Products in Aerosols from  $\alpha$ -Pinene Ozonolysis and the Boreal Forest. *Environ. Sci. Technol. Lett.* **2016**, *3*, 280–285.
- (50) Makowski, M. J.; Stern, A. C.; Hemminger, J. C.; Tobias, D. J. Orientation and Structure of Acetonitrile in Water at the Liquid–Vapor Interface: A Molecular Dynamics Simulation Study. *J. Phys. Chem. C* **2016**, *120*, 17555–17563.
- (51) Perrine, K. A.; Van Spyk, M. H.; Margarella, A. M.; Winter, B.; Faubel, M.; Bluhm, H.; Hemminger, J. C. Characterization of the Acetonitrile Aqueous Solution/Vapor Interface by Liquid-Jet X-Ray Photoelectron Spectroscopy. *J. Phys. Chem. C* **2014**, *118*, 29378–29388
- (52) Enami, S.; Sakamoto, Y. OH-Radical Oxidation of Surface-Active Cis-Pinonic Acid at the Air—Water Interface. *J. Phys. Chem. A* **2016**, 120, 3578—3587.
- (53) Donaldson, D. J.; Anderson, D. Adsorption of Atmospheric Gases at the Air-Water Interface. 2. C<sub>1</sub>-C<sub>4</sub> Alcohols, Acids, and Acetone. *J. Phys. Chem. A* **1999**, *103*, 871–876.
- (54) Enami, S.; Fujii, T.; Sakamoto, Y.; Hama, T.; Kajii, Y. Carboxylate Ion Availability at the Air-Water Interface. *J. Phys. Chem. A* **2016**, *120*, 9224–9234.

- (55) Houriez, C.; Meot-Ner, M.; Masella, M. Simulated Solvation of Organic Ions II: Study of Linear Alkylated Carboxylate Ions in Water Nanodrops and in Liquid Water. Propensity for Air/Water Interface and Convergence to Bulk Solvation Properties. *J. Phys. Chem. B* **2015**, *119*, 12094–12107.
- (56) Gilman, J. B.; Eliason, T. L.; Fast, A.; Vaida, V. Selectivity and Stability of Organic Films at the Air-Aqueous Interface. *J. Colloid Interface Sci.* **2004**, 280, 234–243.
- (57) Boand, G.; Houriet, R.; Gaumann, T. Gas-Phase Acidity of Aliphatic-Alcohols. J. Am. Chem. Soc. 1983, 105, 2203-2206.
- (58) Caldwell, G.; Renneboog, R.; Kebarle, P. Gas-Phase Acidities of Aliphatic Carboxylic-Acids, Based on Measurements of Proton-Transfer Equilibria. *Can. J. Chem.* 1989, 67, 611–618.
- (59) Limbeck, A.; Kulmala, M.; Puxbaum, H. Secondary Organic Aerosol Formation in the Atmosphere Via Heterogeneous Reaction of Gaseous Isoprene on Acidic Particles. *Geophys. Res. Lett.* **2003**, *30*, 1996.
- (60) Liggio, J.; Li, S. M.; Brook, J. R.; Mihele, C. Direct Polymerization of Isoprene and Alpha-Pinene on Acidic Aerosols. *Geophys. Res. Lett.* **2007**, *34*, L05814.
- (61) Connelly, B. M.; Tolbert, M. A. Reaction of Isoprene on Thin Sulfuric Acid Films: Kinetics, Uptake, and Product Analysis. *Environ. Sci. Technol.* **2010**, *44*, 4603–4608.
- (62) Matsuoka, K.; Sakamoto, Y.; Hama, T.; Kajii, Y.; Enami, S. Reactive Uptake of Gaseous Sesquiterpenes on Aqueous Surfaces. *J. Phys. Chem. A* **2017**, *121*, 810–818.
- (63) Enami, S.; Mishra, H.; Hoffmann, M. R.; Colussi, A. J. Protonation and Oligomerization of Gaseous Isoprene on Mildly Acidic Surfaces: Implications for Atmospheric Chemistry. *J. Phys. Chem. A* **2012**, *116*, 6027–6032.
- (64) Enami, S.; Hoffmann, M. R.; Colussi, A. J. Dry Deposition of Biogenic Terpenes Via Cationic Oligomerization on Environmental Aqueous Surfaces. *J. Phys. Chem. Lett.* **2012**, *3*, 3102–3108.
- (65) Pye, H. O.; Murphy, B. N.; Xu, L.; Ng, N. L.; Carlton, A. G.; Guo, H.; Weber, R.; Vasilakos, P.; Appel, K. W.; Budisulistiorini, S. H.; et al. On the Implications of Aerosol Liquid Water and Phase Separation for Organic Aerosol Mass. *Atmos. Chem. Phys.* **2017**, *17*, 343–369.
- (66) Guo, H.; et al. Fine Particle pH and the Partitioning of Nitric Acid During Winter in the Northeastern United States. *J. Geophys. Res. Atmos.* **2016**, *121*, 10355–10376.
- (67) Bougiatioti, A.; Nikolaou, P.; Stavroulas, I.; Kouvarakis, G.; Weber, R.; Nenes, A.; Kanakidou, M.; Mihalopoulos, N. Particle Water and pH in the Eastern Mediterranean: Source Variability and Implications for Nutrient Availability. *Atmos. Chem. Phys.* **2016**, *16*, 4579–4591.
- (68) Guo, H.; et al. Fine-Particle Water and pH in the Southeastern United States. *Atmos. Chem. Phys.* **2015**, *15*, 5211–5228.
- (69) Guo, H.; Liu, J.; Froyd, K. D.; Roberts, J. M.; Veres, P. R.; Hayes, P. L.; Jimenez, J. L.; Nenes, A.; Weber, R. J. Fine Particle pH and Gas-Particle Phase Partitioning of Inorganic Species in Pasadena, California, During the 2010 CalNex Campaign. *Atmos. Chem. Phys.* 2017, 17, 5703–5719.
- (70) Fang, T.; Guo, H.; Zeng, L.; Verma, V.; Nenes, A.; Weber, R. J. Highly Acidic Ambient Particles, Soluble Metals, and Oxidative Potential: A Link between Sulfate and Aerosol Toxicity. *Environ. Sci. Technol.* **2017**, *51*, 2611–2620.
- (71) Enami, S.; Sakamoto, Y.; Colussi, A. J. Fenton Chemistry at Aqueous Interfaces. *Proc. Natl. Acad. Sci. U. S. A.* **2014**, *111*, 623–628.
- (72) Enami, S.; Colussi, A. J. Long-Range Hofmeister Effects of Anionic and Cationic Amphiphiles. *J. Phys. Chem. B* **2013**, *117*, 6276–6281.
- (73) Enami, S.; Hoffmann, M. R.; Colussi, A. J. Proton Availability at the Air/Water Interface. *J. Phys. Chem. Lett.* **2010**, *1*, 1599–1604.
- (74) Enami, S.; Colussi, A. J. Long-Range Specific Ion-Ion Interactions in Hydrogen-Bonded Liquid Films. *J. Chem. Phys.* **2013**, 138, 184706.
- (75) Enami, S.; Vecitis, C. D.; Cheng, J.; Hoffmann, M. R.; Colussi, A. J. Electrospray Mass Spectrometric Detection of Products and

- Short-Lived Intermediates in Aqueous Aerosol Microdroplets Exposed to a Reactive Gas. J. Phys. Chem. A 2007, 111, 13032-13037.
- (76) Enami, S.; Hoffmann, M. R.; Colussi, A. J. How Phenol and Alpha-Tocopherol React with Ambient Ozone at Gas/Liquid Interfaces. *J. Phys. Chem. A* **2009**, *113*, 7002–7010.
- (77) Enami, S.; Vecitis, C. D.; Cheng, J.; Hoffmann, M. R.; Colussi, A. J. Global Inorganic Source of Atmospheric Bromine. *J. Phys. Chem.* A 2007, 111, 8749–8752.